15

Application of cerium oxide nanopowders for silicon polishing

© N.I. Chkhalo,[1] A.A. Akhsakhalyan,[1] Yu.A. Vainer,[1] M.V. Zorina,[1] A.E. Pestov,[1] M.V. Svechnikov,[1] M.N. Toropov,[1] N. Kumar,[1] Yu.M. Tokunov[2]

[1] Institute of Physics of Microstructures, Russian Academy of Sciences,
607680 Nizhny Novgorod, Russia
[2] MIPT,
141701 Dolgoprudny, Moscow oblast, Russia
e-mail: chkhalo@ipm.sci-nnov.ru

Received April 2, 2021
Revised April 2, 2021
Accepted April 2, 2021

The research methods and the first results obtained in the study of the roughness of single-crystal silicon (111) substrates processed at the final stage by various methods are described: traditional polishing without the use of chemical-mechanical polishing (CMP), with the use of CMP and without CMP, but with the use of oxide cerium nanopowders. The efficiency of using CeO_2 nanopowders has been demonstrated. The following effective roughness values were obtained: without CMP - 3.56 nm, with CMP - 0.54 nm, and without CMP, but with CeO_2 polishing - 0.93 nm.

Keywords: Surface, roughness, X-ray optics, deep grinding-polishing.

DOI: 10.21883/TP.2022.13.52236.95-21

Introduction

Recently due to modernization of the 3rd generation synchrotrons and appearance of free electron lasers and 4th generation synchrotrons, including actively developed in our country SKIF (the Siberian ring source of photons) [1], the problem of mirrors radiation stability became more relevant. For these applications there is another condition related to necessity of maintaining the coherent properties of original beam. Therefore, the thermally-induced deformations of mirrors shape enter the picture. The following discussions can be used for evaluation of permissible shape deformations. To provide images diffracting quality it is necessary that the reflected beam phase during reflection in each local incidence point does not change more than by quarter of wavelength. Considering grazing incidence of radiation to mirror this condition can be rewritten as

$$\Delta X < \lambda/4(\sin\theta)^{-1}, \quad (1)$$

where ΔX is local deflection of mirror profile from calculated, λ is wavelength and θ is grazing incidence angle. For mirrors with multilayer coatings, increasing mirrors operating angles several-fold [2–4], considering Bragg condition the expression (1) can be rewritten as

$$\Delta X < D/2, \quad (2)$$

where D is multilayer mirror period. For significant periods, often used W/B4C multilayer mirrors $D = 2$ nm [5]. Permissible error lies in subnanometer area.

To maintain the high reflection coefficients the substrates microroughness should be less than interlayer roughness in multilayer mirrors, that in case of W/B4C is about 0.2 nm [6].

As theoretical calculations (fully proved to be practically relevant) have shown, only single-crystal silicon can be used as substrates material to minimize the thermally-induced shape deformations. Other materials, including silicon carbide and metals (copper, aluminum, beryllium), are significantly inferior to it in terms of their thermal and physical characteristics [7,8].

Currently the most common method of making the high-precision, including silicon aspheric substrates for mirrors, is the combination of diamond turning and correction of local shape defects with small-size ion beams [9–12]. Polishing with small-size polishers using computer control is used as an alternative to the diamond turning [13]. However, during such processing the roughness is increased in the range of spatial frequencies of $10^{-3} - 1\,\mu\text{m}^{-1}$, called mid-frequency and caused by a tool slapping, and this influences the resolving power of X-ray optics systems the most [14]. Therefore, the best results in terms of accuracy of silicon substrates making were achieved using the technology called Computer-controlled elastic emission machining [15]. This technology as a polishing tool uses localized suspension jet supplied under pressure of 100 atm. Beside the high level of processing controllability, due to lack of the normal component of pressure on abrasive grains in suspension, that always presents during traditional grinding-polishing, this method does not result in damaged layer due to cracking of substrate surface areas. Japanese company JTEC CORPORATION, that mastered this technology, is basically the monopolist in high-precision silicon substrates manufacturing for synchrotron applications [16].

In the last few years we develop two-stage approach for high-precision substrates manufacturing for mirrors of

diffracting quality in X-ray range. It is well known that during grinding-polishing of flat and spherical surfaces the mutual lapping helps to achieve the best quality of optical surfaces processing [17]. Therefore, at the first stage the spherical (flat) substrates with curve radius, closest to the required asphere, are manufactured using lapping method. At the second stage the correction of local defects and shape asphericization are performed using specially designed ion-beam etching unit [18].

High controllability of ion-beam machining process allows to create high-precision surfaces with highly complex asphere shape, and, as a result, to develop unique optical schemes, implementation of which was not possible earlier [19,20]. However, for successful implementation of this approach it is necessary to make highly smooth substrates at the first stage, since ion beams smooth down high-frequency roughness fairly well and almost do not impact on the mid-frequency roughness, starting from frequencies of $0.2-0.3\,\mu m^{-1}$ [21,22]. In [23] the suspensions with micropowders of CeO_2 were studied on substrates of fused silica. These powders demonstrated their high efficiency. On significantly steep spherical substrate with diameter of 100 mm and curve radius of 137.5 mm, the numerical aperture NA = 0.36, the effective roughness of about 0.2 nm in frequency range of $0.025-65\,\mu m^{-1}$ was achieved. At the same time the shape accuracy was achieved: maximum level difference MP = 16 nm and mean square deviation CKO = 3.3 nm ($\approx \lambda/200$). After ion polishing the effective roughness was dropped to about 0.1 nm, that is sufficient for X-ray optics of diffracting quality.

The purpose of this study was to research the possibilities of this technology and micropowders use for single-crystal silicon polishing.

1. Experimental procedure

1.1. Mechanical lapping procedure

As in [23], the lapping machine D-150 was used. Surface treatment was performed using pitch polisher (SP5 resin). At the early stage of lapping the same suspension based on water solution of cerium oxide micropowders, made by MFTI (Dolgoprudny), with grain size of $0.1-0.3$ and $0.05-0.1\,\mu m$ was used. At the final stage the suspension, made as per advanced process flow, with adding of CeO_2 nanopowder fraction with particles size of 19 nm was used. Fig. 1 shows the powder particles size distribution. As can be seen in the figure, the distribution is bimodal with peaks of 22 and 108 nm.

The processed substrate, picture of which is presented in Fig. 2, was a rectangular block of single-crystal silicon (111) with dimensions of $15 \times 25 \times 120$ mm. The crystallographic orientation of (111) was selected with potential for the further ion-beam etching to reduce high-frequency roughness, since Si (111) surface can be efficiently smoothed with perpendicular etching.

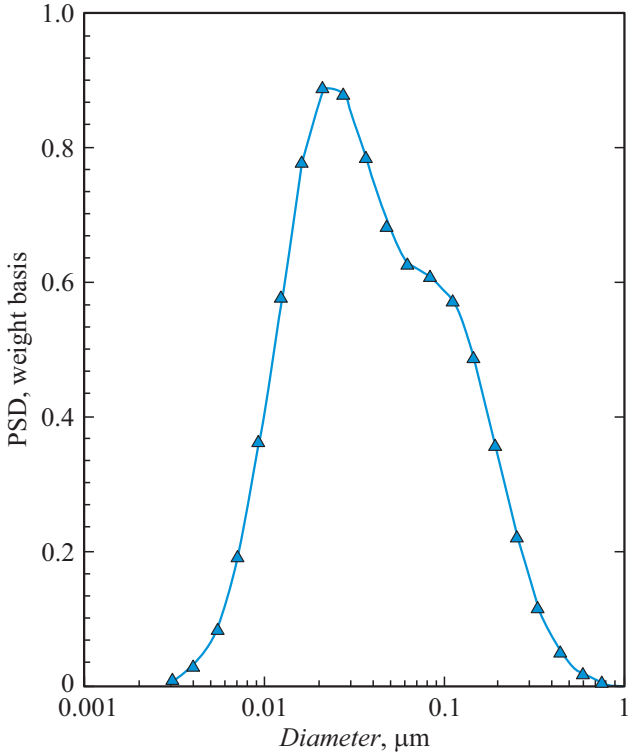

Figure 1. CeO_2 powder size distribution in advanced suspension.

Figure 2. Picture of processed substrate.

1.2. Roughness measurement methods

Statistical properties of surface roughness and damaged layer depth were the subjects of research. As noticed in other studies, for instance in [24], the supersmooth surfaces roughness study has some specifics, requiring critical approach during analysis of actual possibilities of

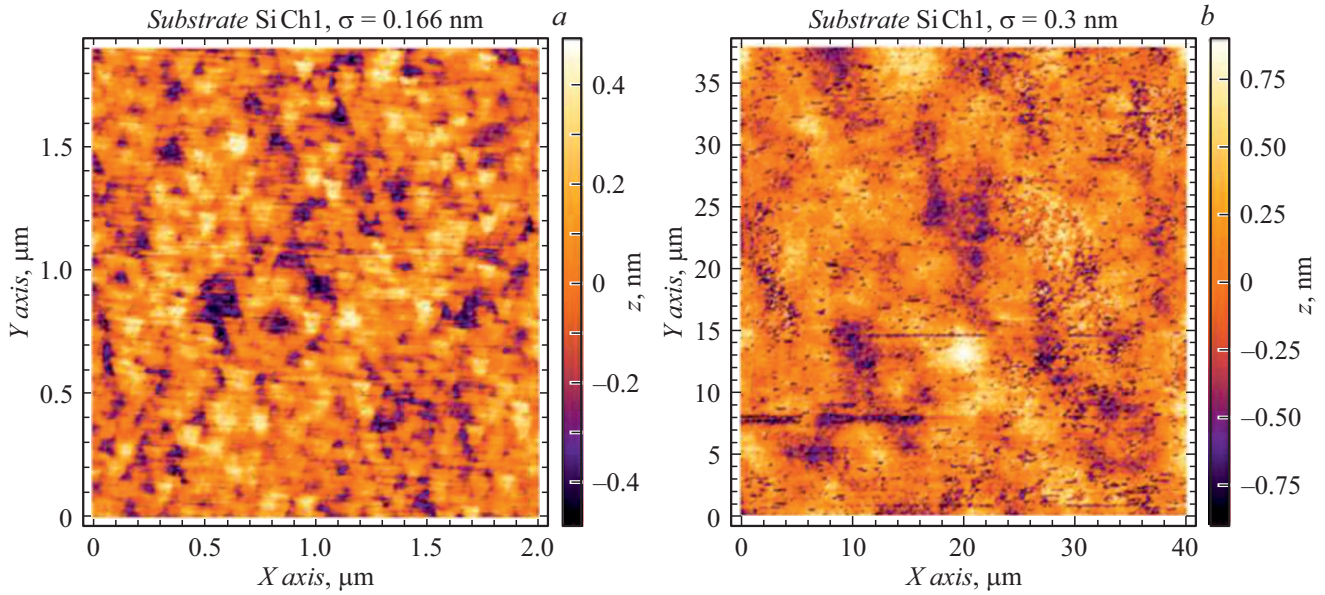

Figure 3. AFM images of silicon surface for microelectronics industry after CMP.

devices and methods in use. Particularly, the widely used white light interferometry method [25,26] gives satisfactory results only for surfaces with effective roughness of above 1 nm [21]. Presence of damaged layer, that results in additional scattering on volume inhomogeneities [29], significantly influences the diffuse X-ray scattering (DXRS) spectra [27,28]. Atomic force microscopy (AFM) [30] is affected by scanner nonlinearity, that appears at bigger, above $10\,\mu$m, frames [21]. Mechanical stiffness of cantilever beam significantly influences the results of measurements. Also, during AFM measurements the noises, that depend not only on characteristics of device in use, but also on external conditions, should be considered [31]. Therefore, we recognize the roughness measurement results as valid, if roughness power spectral density (PSD) functions, measured using various methods, match together in the area of their operating ranges crossing.

Methods of mirror and diffuse scattering of X-ray radiation and AFM were used in this study. Value and angle distribution of DXRS are mainly defined by dispersive relief frequency spectrum. If condition of low roughness and grazing angle is met,

$$k\sigma \sin\theta_0 \ll 1; \quad k\sigma|\varepsilon_+ - \cos\theta_0|^{1/2}, \tag{3}$$

where k is wave number, σ is root-mean-square roughness, θ_0 is probing beam grazing angle, meaning, that wave field changes a little at $\pm\sigma$ scale from scattering boundary [27], then for scattering intensity, integrated over azimuthal angle, the following expression can be written

$$\Pi(\theta, \theta_0) = \frac{k^5}{16\pi k_-(q_0)\sqrt{q_0 q}} \times \left| \int \psi_0(z, q_0)\psi_0(z, q)\varepsilon'(z)dz \right|^2 \mathrm{PSD}_{1D}(p), \tag{4}$$

where θ is scattering angle $q_0 = k\cos\theta_0$, $q = k\cos\theta$, $\psi_0(z, q)$ are field distribution in structure, $\mathrm{PSD}_{1D}(p)$ is one-dimensional power spectral density of relief, p is spatial frequency.

In case of scattering on single surface with sharp drop ε

$$\Pi(\theta, \theta_0) = \frac{k^3|1-\varepsilon|^2}{16\pi \sin\theta_0} |t(\theta_0)t(\theta)|^2 \mathrm{PSD}_{1D}(p), \tag{5}$$

where $t(\theta)$ is Fresnel transmission coefficient.

It is important that regardless of near-surface layer structure the scattering intensity consists of two multipliers — electrodynamical factor — function of one-dimensional layered geometry of structure, wavelength and experiment geometry — and roughness spectrum. If electrodynamical factor is known, the required spectrum is calculated by simple division of experimentally measured intensity (considering instrumental function) by this multiplier:

$$\mathrm{PSD}_{1D}(p) = \Pi_{\exp}(\theta, \theta_0) \Big/ \frac{k^2}{16\pi k_-(q_0)\sqrt{q_0 q}} \times \left| \int \psi_0(z, q_0)\psi_0(z, q)\varepsilon'(z)dz \right|^2. \tag{6}$$

Experiment geometry is known a priori, one-dimensional layered structure of sample is defined upon the results of reflection and diffuse scattering curves fitting using premodel PSD.

Effective roughness σ_{eff} of surface is defined from

$$\sigma_{\text{eff}}^2 = \int_{p_{\min}}^{p_{\max}} \mathrm{PSD}_{1D}(p)dp, \tag{7}$$

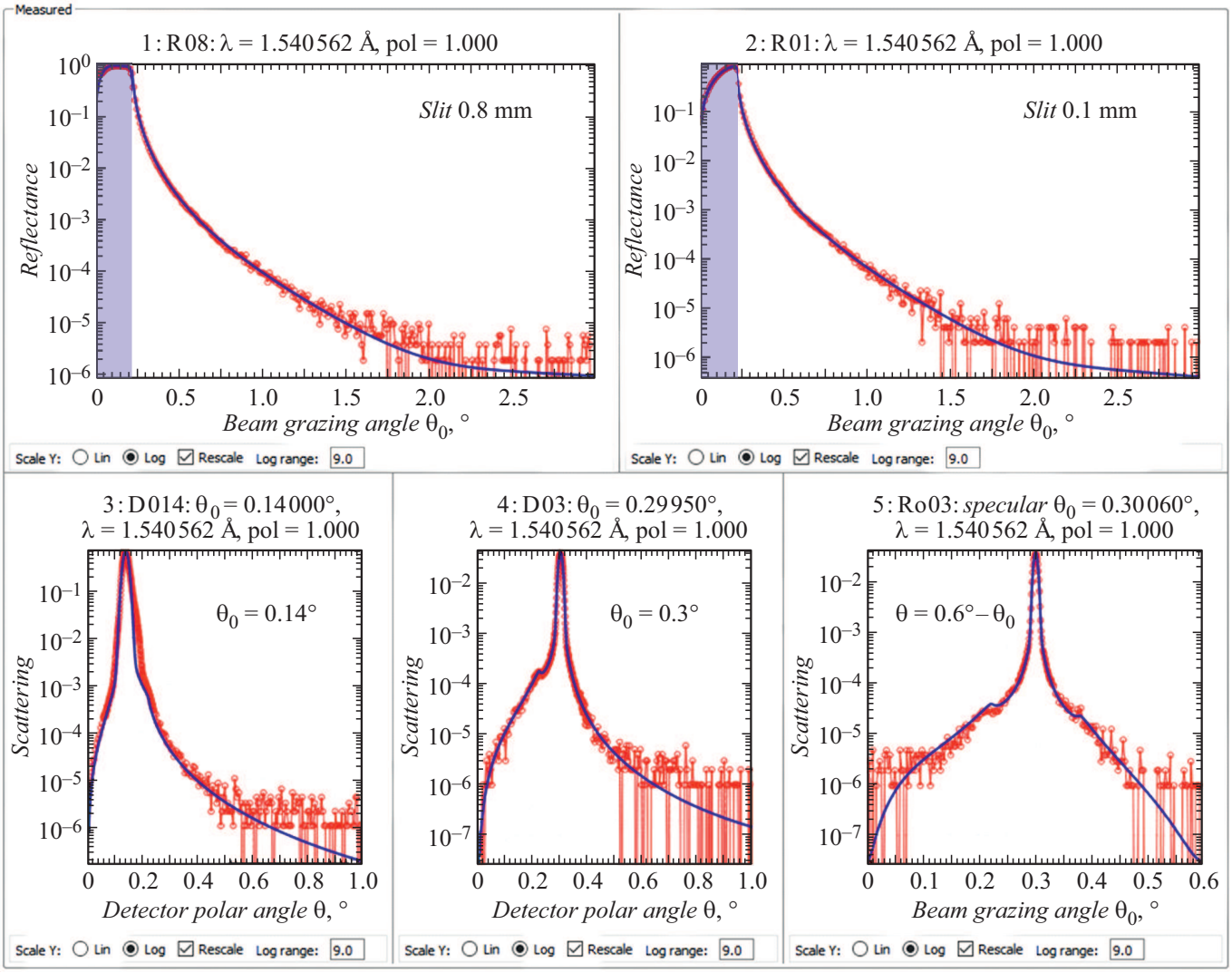

Figure 4. Curves of mirror reflection (top), measured with various slits on detector, of diffuse scattering (bottom) for the sample under research.

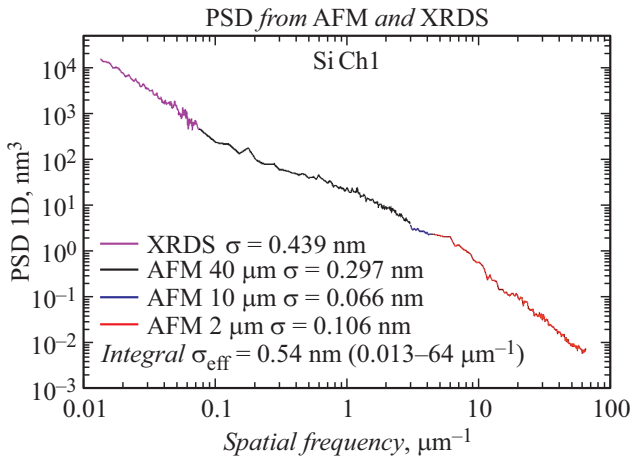

Figure 5. PSD function of roughness, built using data of AFM and DXRS.

where p_{min} and p_{max} are minimum and maximum spatial frequencies, in interval between which the PSD function is located.

2. Experimental results

Initially the standard silicon plate for microelectronics industry after chemical-mechanical polishing (CMP) was studied as a „reference“ for comparison. It is known that such method allows to make the smoothest substrates with completely removed damaged layer. The only disadvantage of this silicon polishing technology with regard to X-ray optics tasks is unsatisfactory precision of surface shape due to usage of polishers of „soft“ materials and complexity of its control during chemical etching. However, in terms of roughness and damaged layer, this can be considered as a reference.

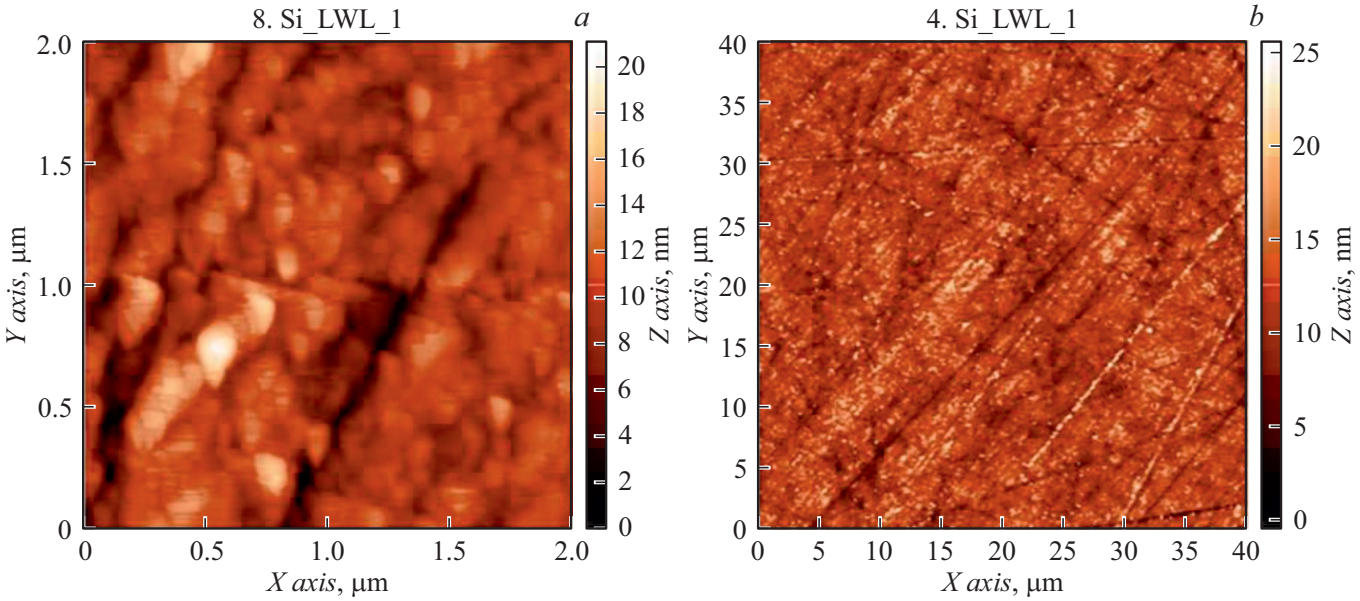

Figure 6. AFM images of the studied sample surface after DGP without CMP.

Fig. 3 and 4 show AFM images and curves of mirror reflection (Fig. 4, top) and diffuse scattering (Fig. 4, bottom) for the studied sample.

Modeling of X-ray reflection and scattering curves was performed using Multifitting software [32]. It can be observed that the curves are well modelled. There is a small difference in the area of reflected beam at grazing angle of 0.14°. But the reason behind this difference is thin plate curving, inevitable when fastening, and this effect increases with angle reduction.

Roughness power spectral density function, presented in Fig. 5, was built using AFM and DXRS data. Beside integral roughness the figure also includes effective roughness as areas under the corresponding parts of PSD function. This effective roughness is not a complete roughness for the corresponding frame, it corresponds only to a part of PSD presented on diagram.

Surface effective roughness after CMP in a frequency range of $0.013-64\,\mu\text{m}^{-1}$ was about 0.54 nm. It should be noted that near-matching values were observed during studying of Si plates after CMP for microelectronics industry in [33]. Good stitching of PSD functions, observed under both methods, confirms that scattering is mainly defined by surface, not damaged layer.

Similar measurements were performed for the experimental sample after standard deep grinding-polishing (DGP). At grinding stage the boron carbide micropowders with grain size of $14\,\mu$m in the beginning and $7\,\mu$m in the end were used. After boron carbide the fine grinding and polishing were performed using diamond micropowders with grain size, varying from $5\,\mu$m to submicrometer. The final polishing was finished with polirit. It should be noted that DGP procedure was performed on „solid“ pitch polishers to provide reliable lapping and high quality of surface evenness. AFM measurement results are presented in Fig. 6, X-ray — in Fig. 7. Function of roughness power spectral density, built using AFM and DXRS data, is presented in Fig. 8.

As shown in the figures, effective roughness of silicon substrate after DGP, but without CMP, is significantly inferior to substrates after CMP and does not meet the requirements for X-ray mirrors. Effective roughness in a frequency range of $0.0073-64\,\mu\text{m}^{-1}$ was 3.56 nm.

After researches the lapping procedure was performed using suspensions based on cerium oxide nanopowders described in the beginning of the paper. Lapping was also performed using pitch polisher for 2 h. Measurement results are presented in Figs. 9–11.

Based on presented experimental data, application of suspension with CeO_2 nanopowders at final stage reduced roughness almost by a factor of 4, lowering it to sub-nanometer level. Effective roughness in a frequency range of $0.0125-64\,\mu\text{m}^{-1}$ was about 0.93 nm.

3. Results discussion and main conclusions

This study includes comparison of surface roughness of substrates of single-crystal silicon, exposed to standard DGP with use of abrasives based on boron carbide, diamond micropowders and polirit, but with different treatment at final stage. The first method (with CMP use), as expected, allows to make substrates with roughness, corresponding to the requirements to substrates for X-ray mirrors. The main problem of CMP is practical impossibility of making the

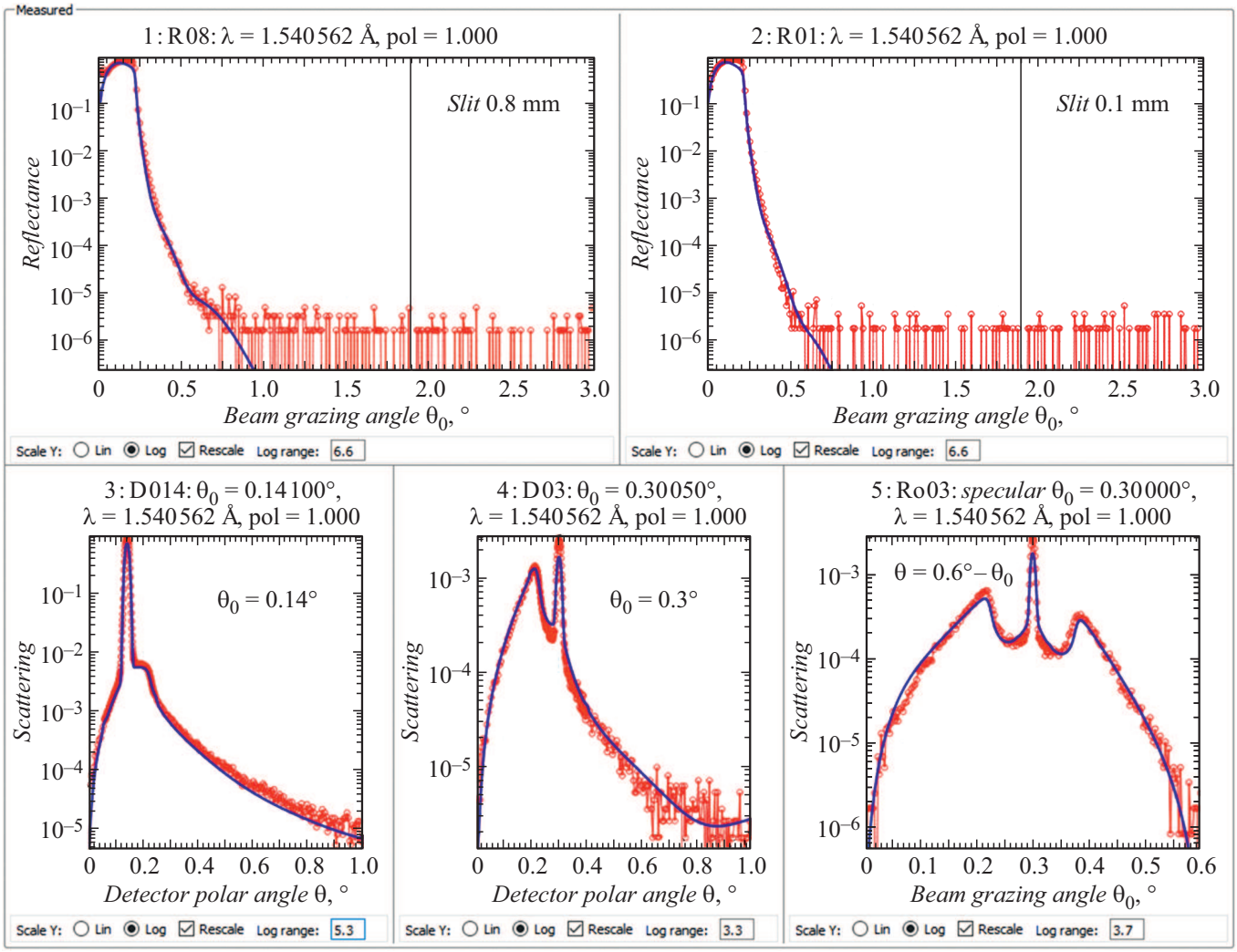

Figure 7. Curves of mirror reflection (top), measured with various slits on detector, of diffuse scattering (bottom) for the sample under research after DGP without CMP.

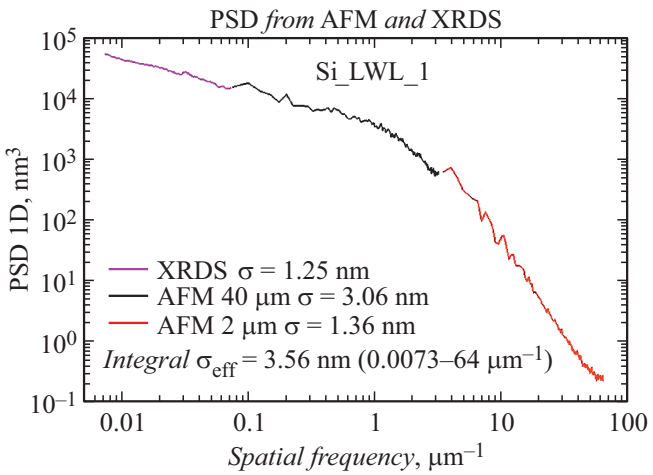

Figure 8. PSD function of roughness, built using data of AFM and DXRS.

high-accuracy surfaces due to usage of „soft“ polishers and high etching rate.

Substrate, made by DGP method without CMP, but with pitch polishers using, showed the high level of roughness, about 3.56 nm in a spatial frequencies range of $0.0073-64\,\mu m^{-1}$, that prevents its use in X-ray optics. We also experience a problem with adequate description of DXRS and reflection curves under perturbation theory regarding roughness height due to non-observance of condition (3) because of high roughness. Accurate description under any parameters of incoming radiation and roughness is possible using strict electromagnetic theory [34-36].

Application of finished machining using suspension based on cerium oxide nanopowders for this substrate significantly improved surface quality. Effective roughness reduced to 0.93 nm. For comparison, with CMP the roughness was 0.54 nm.

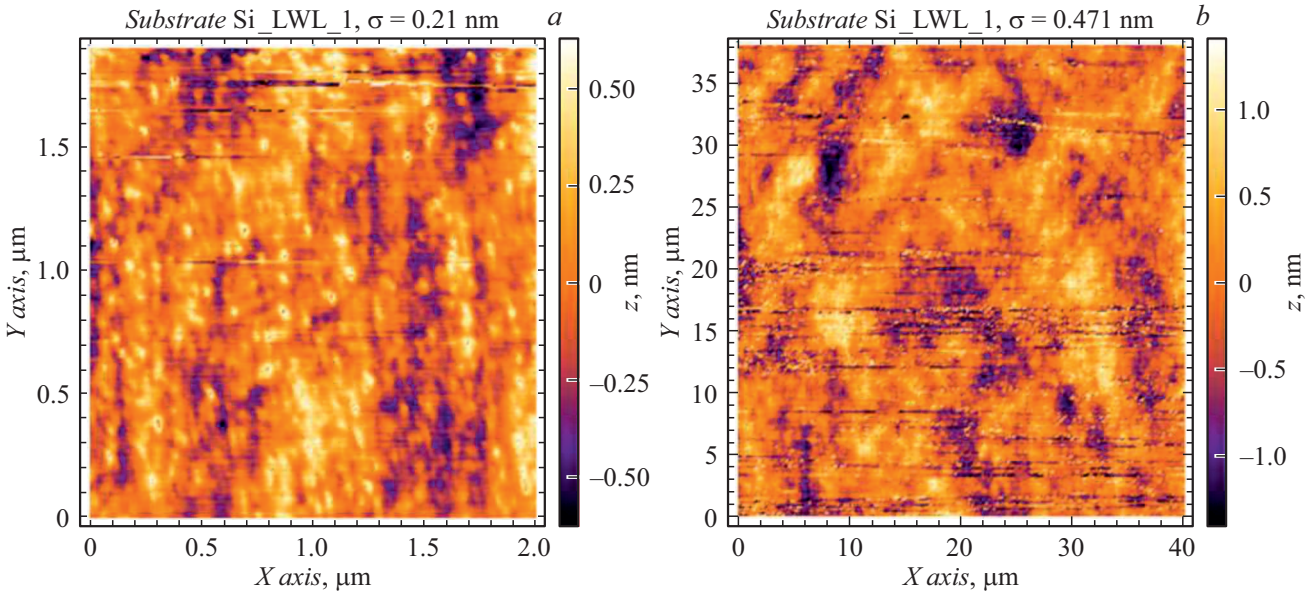

Figure 9. AFM images of the studied sample surface after DGP without CMP and with finished machining using CeO_2 nanopowders.

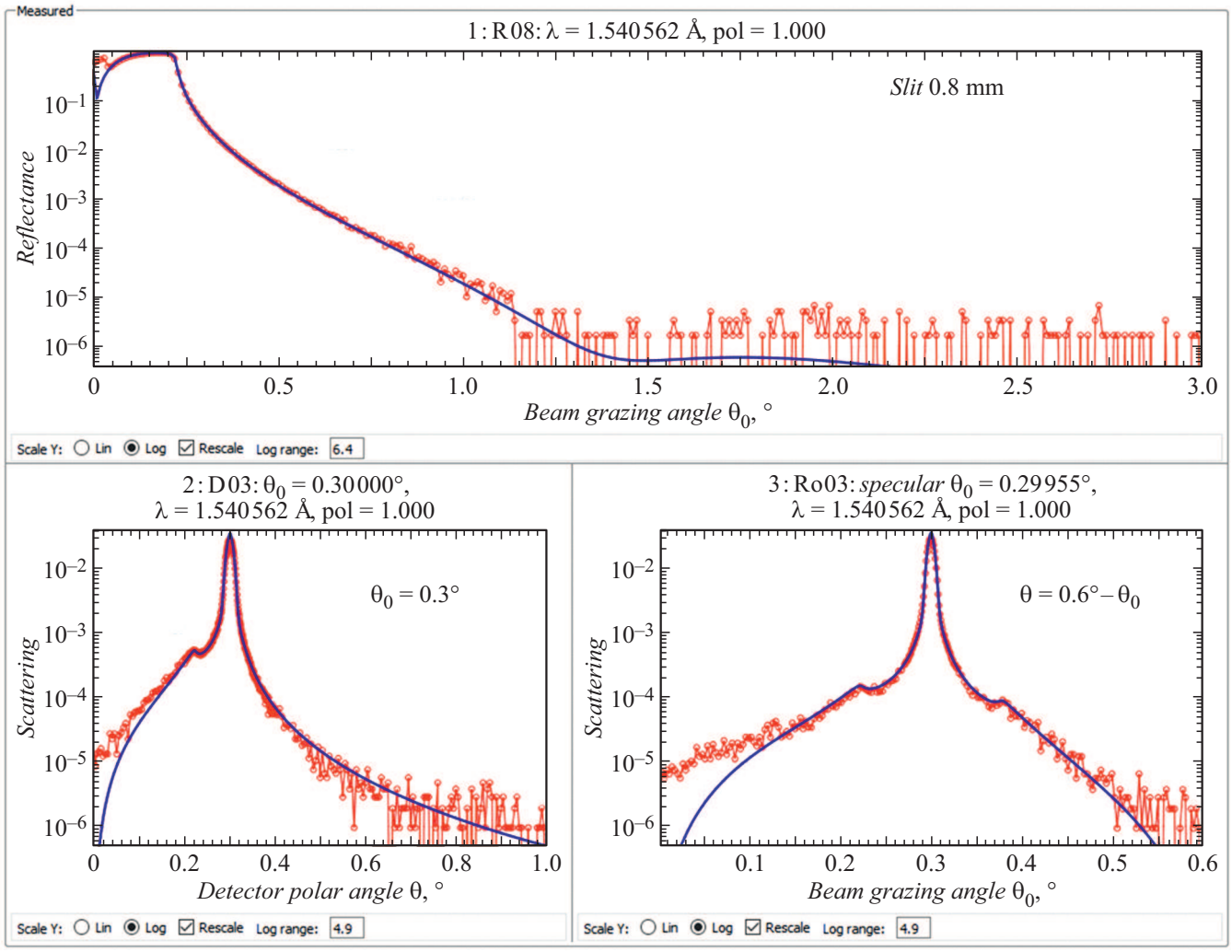

Figure 10. Curves of mirror reflection (top), measured with various slits on detector, of diffuse scattering (bottom) for the sample under research after DGP without CMP, but with finished machining using CeO_2 nanopowders.

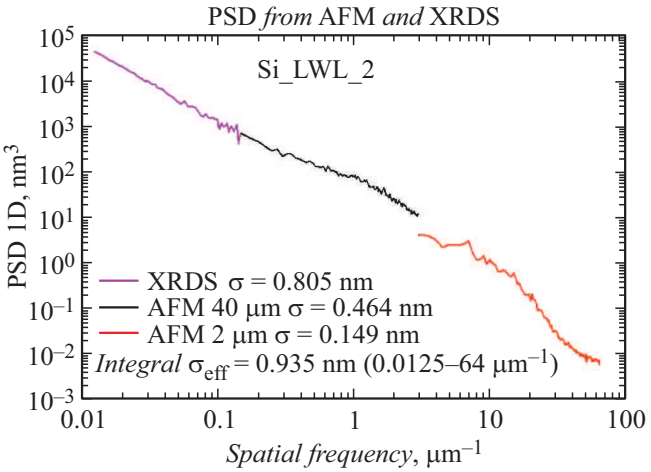

Figure 11. PSD function of roughness, built using data of AFM and DXRS.

Conclusion

Thus the conceptual possibility of making the single-crystal silicon substrates using mechanical lapping method without CMP with subnanometer roughness, that is closer to the requirements for X-ray optics applications, is shown. The further steps will be directed to optimization of process parameters: selection of resin type, treatment temperature, treatment time, ion-beam polishing to achieve or even surpass the characteristics of silicon substrates with CMP.

Acknowledgements

The study was performed with the support of RSF, Agreement №21-72-20108.

Conflict of interest

The authors declare that they have no conflict of interest.

References

[1] S.V. Rashchenko, M.A. Skamarokha, G.N. Baranov, Y.V. Zubavichus, Ia.V. Rakshun. AIP Conf. Proceed., **2299**, 060001 (2020). DOI: org/10.1063/5.0030346
[2] G. Admans, P. Berkvens, A. Kaprolat, J.-L. Revol. ESRF upgrade programme phase II (2015–2022). Technical design study. (Imprimerie de Pont de Claix © ESRF, 2014) p. 192. http://www.esrf.eu/Apache_files/Upgrade/ESRF-orange-book.pdf.
[3] Electronic resource. Access mode: https://www.maxiv.lu.se/about-us/
[4] A. Erko, M. Idir, Th. Krist, A.G. Michette. *Modern Developments in X-ray and Neutron Optics* (Springer Berlin Heidelberg, N Y., 2008), p. 533. ISBN 978-3-540-74560-0
[5] Ch. Morawe, R. Barrett, K. Friedrich, R. Klünder, A. Vivo. J. Phys.: Conf. Series, 425, 052027 (2013). DOI: 10.1088/1742-6596/425/5/052027
[6] S.S. Andreev, M.S. Bibishkin, N.I. Chkhalo, E.B. Kluenkov, K.A. Prokhorov, N.N. Salashchenko, M.V. Zorina, F. Schafers, L.A. Shmaenok. J. Synchrotron Radiation, **10** (5), 358 (2003). DOI: 10.1107/S0909049503015255
[7] P.Z. Takacs. Synchrotron Radiation News, **2** (26), 24 (1989).
[8] N.I. Chkhalo, M.V. Zorina, I.V. Malyshev, A.E. Pestov, V.N. Polkovnikov, N.N. Salashchenko, D.S. Kazakov, A.V. Mil'kov, I.L. Strulya. ZhTF, **89** (11), 1686 (2019). DOI: 10.21883/JTF.2019.11.48329.134-19
[9] H. Thiess, H. Lasser, F.Siewert. Nucl. Instrum. Methods Phys. Res. A, **616**, 157 (2010). DOI: 10.1016/j.nima.2009.10.077
[10] K.N. Khatri, R. Sharma, V. Mishra, H. Garg, V. Karar. Advan. Mater. Proceed., **2** (7), 425 (2017). DOI: 10.5185/amp.2017/704
[11] L.N. Abdulkadir, K. Abou-El-Hossein, A.I. Jumare, P.B. Odedeyi, M.M. Liman, T.A. Ola niyan. Int. J. Adv. Manuf. Technol., **96**, 173 (2018). DOI: 10.1007/s00170-017-1529-x
[12] T. Arnold, G. Bohm, R. Fechner, J. Meister, A. Nickel, F. Frost, T. Hansel, A. Schindler. Nucl. Instrum. Methods Phys. Res., A **616**, 147 (2010). DOI: 10.1016/J.NIMA.2009.11.013
[13] M.A. Okatov, E.A. Antonov, A. Baygozhin, M.I. Bakaev, I.V. Belova, I.Ya. Bubis, V.A. Veydenbakh, N.M. Vorontsova, S.V. Danilov, N.Yu. Dudkina, I.I. Dukhopel, S.M. Kuznetsov, Z.A. Kukleva, G.V. Listratova, B.I. Lodygin, Yu.K. Lysyany, S.V. Lyubarsky, A.V. Mikhaylov, V.Ya. Nazarova, E.I. Ponfilenok, B.I. Petrov, G.T. Petrovsky, V.P. Poveshchenko, G.D. Pridatko, S.M. Prokhorchik, V.N. Savushkin, R.S. Sokolova, N.V. Suykovskaya, L.V. Tarnovskaya, I.D. Torbin, L.A. Cherezova, B.A. Chunin, A.V. Shatilov, E.I. Shepurev, Z.V. Shirokshina, V.Kh. Yagmurov. *Spravochnik tekhnologa-optika*, pod red. M.A. Okatova. (Politekhnika, SPb, 2004), s. 679 (in Russian).
[14] U. Dinger, F. Eisert, H. Lasser, M. Mayer, A. Seifert, G. Seitz, S. Stacklies, F.-J. Stickel, M. Weiser. Proceed. SPIE, **4146**, 35 (2000). DOI: 10.1117/12.406674
[15] K. Yamauchi, H. Memura, K. Inagaki, Y. Mori. Rev. Sci. Instrum., **73** (11), 4028 (2002). DOI: 10.1063/1.1510573
[16] Electronic resource. Access mode: https://www.j-tec.co.jp/english/optical/
[17] V.A. Smirnov. *Obrabotka opticheskogo stekla* (Mashinostroenie, L., 1980), s. 183 (in Russian).
[18] N.I. Chkhalo, I.A. Kaskov, I.V. Malyshev, M.S. Mikhaylenko, A.E. Pestov, V.N. Polkovnikov, N.N. Salashchenko, M.N. Toropov, I.G. Zabrodin. Precision Engineer., **48**, 338 (2017). DOI: http://dx.doi.org/10.1016/j.precisioneng.2017.01.004
[19] M.N. Brychikhin, N.I. Chkhalo, Ya.O. Eikhorn, I.V. Malyshev, A.E. Pestov, Yu.A. Plastinin, V.N. Polkovnikov, A.A. Rizvanov, N.N. Salashchenko, I.L. Strulya, M.N. Toropov. Appl. Optics, **55** (16), 4430 (2016). DOI: 10.1364/AO.55.004430
[20] N.I. Chkhalo, I.V. Malyshev, A.E. Pestov, V.N. Polkovnikov, N.N. Salashchenko, M.N. Toropov, S.N. Vdovichev, I.L. Strulya, Yu.A. Plastinin, A.A. Rizvanov. J. Astronom.Telescop., Instrum., Systems, **4** (1), 014003-1-014003-9 (2018). DOI: 10.1117/1.JATIS.4.1.014003
[21] N.I. Chkhalo, S.A. Churin, A.E. Pestov, N.N. Salashchenko, Yu.A. Vainer, M.V. Zorina. Opt. Express, **22** (17), 20094 (2014). DOI: 10.1364/OE.22.020094
[22] N.I. Chkhalo, S.A. Churin, M.S. Mikhaylenko, A.E. Pestov, V.N. Polkovnikov, N.N. Salashchenko, M.V. Zorina. Appl. Optics, **55** (6), 1249 (2016). DOI: 10.1364/AO.55.001249

[23] M.N. Toropov, A.A. Akhsakhalyan, M.V. Zorina, N.N. Salashchenko, N.I. Chkhalo, Yu.M. Tokunov. ZhTF, **90** (11), 1958 (2020). DOI: 10.21883/TP.2022.13.52236.95-21
[24] M.M. Barysheva, Yu.A. Vainer, B.A. Gribkov, M.V. Zorina, A.E. Pestov, D.N. Rogachev, N.N. Salashenko, N.I. Chkhalo. Bull. Russ. Academy Sci.: Physics, **75** (1), 67 (2011). DOI: 10.3103/S1062873811010059
[25] R. Blunt. *Proceedings of CEMANTECH Conference* (Vancouver, Canada, April 24–27, 2006), p. 59–62.
[26] D. Martinez-Galarce, R. Soufli, D.L. Windt, M. Bruner, E. Gullikson, Sh. Khatri, E. Spiller, J.C. Robinson, Sh. Baker, E. Prast. Opt. Engineer., **52** (9), 095102-1-14 (2013). DOI: 10.1117/1.OE.52.9.095102
[27] I.V. Kozhevnikov, M.V. Pyatakhin. J. X-ray Sci. Technol., **8** (4), 253 (1998).
[28] V.E. Asadchikov, I.V. Kozhevnikov, Yu.S. Krivonosov, R. Mercier, T.H. Metzger, C. Morawe, E. Ziegler. Nucl. Instrum. Meth. Phys. Res. A, **530**, 575 (2004). DOI: 10.1016/J.NIMA.2004.04.216
[29] M.M. Barysheva, N.I. Chkhalo, M.N. Drozdov, M.S. Mikhailenko, A.E. Pestov, N.N. Salashchenko, Yu.A. Vainer, P.A. Yunin, M.V. Zorina. J. X-Ray Sci. Technol., **27** (5), 857 (2019). DOI: 10.3233/XST-190495
[30] J.E. Griffith, D.A. Grigg. J. Appl. Phys., **74** (9), 83 (1993). DOI: 10.1063/1.354175
[31] N.I. Chkhalo, N.N. Salashchenko, M.V. Zorina. Rev. Sci. Instrum., **86**, 016102 (2015). https://doi.org/10.1063/1.4905336
[32] M. Svechnikov. J. Appl. Crystall., **53** (1), 244 (2020). DOI: 10.1107/s160057671901584x
[33] A.R. Belure, A.K. Biswas, D. Raghunathan, Rishipal, S. Bhartiya, R. Singh, S.K. Rai, R.S. Pawade, M.P. Kamath, N.S. Benerji., Mater. Today: Proceed., **26**, 2260 (2020). DOI: 10.1016/j.matpr.2020.02.490
[34] A.V. Andreev. Phys. Lett. A, **219** (5–6), 349 (1996). DOI: 10.1016/0375-9601(96)00469-0
[35] L.I. Goray. J. Appl. Phys., **108** (3), 033516 (2010). DOI: 10.1063/1.3467937
[36] L. Goray. J. Synchrotron Radiat., **28** (1), 196 (2021). DOI: 10.1107/S160057752001440X